

# Varying the Blending Protocol to Control the Morphology of Model Compatibilized Polymer Blends

Jeffrey D. Martin and Sachin S. Velankar

Dept. of Chemical Engineering, University of Pittsburgh, Pittsburgh, PA 15261

DOI 10.1002/aic.11413

Published online January 29, 2008 in Wiley InterScience (www.interscience.wiley.com).

*The structure of an oil/water emulsion is known to depend on its preparation method. Here, we test whether the preparation protocol can be used to control the morphology of “model” blends of immiscible polymers compatibilized by a diblock copolymer. Two preparation protocols were tested. In the “double blending” protocol, a droplet-matrix blend was blended with additional drop-phase fluid. As in oil/water emulsions, this yielded a drop-within-drop “double emulsion” morphology. Coalescence suppression due to compatibilizer was found crucial to double emulsion stability. The rheology of the double emulsion was qualitatively similar to that of a simple droplet-matrix blend, but with an effectively higher drop volume fraction. In the “multistep concentration” protocol, the drop phase was added gradually (rather than all-at-once) to the matrix phase. While this protocol can realize a high-dispersed phase emulsion in oil/water systems, in this case, phase inversion occurred when the drop volume fraction exceeded 0.5. © 2008 American Institute of Chemical Engineers AICHE J, 54: 791–801, 2008*

*Keywords: polymer blends emulsion, morphology, compatibilizer, phase inversion*

## Introduction

An emulsion of oil and water is generally formulated with a small amount of surfactant, which is interfacially-active at the oil/water interface. The surfactant is one of the chief factors determining which phase becomes continuous: with some types of surfactants, the emulsion prefers to have an oil-in-water morphology (or “type”), whereas with other surfactants, a water-in-oil morphology is preferred.<sup>1,2</sup> Mechanistically, the surfactant plays two major roles: (1) it lowers the interfacial tension, thus promoting breakup of drops when the emulsion is prepared, and (2) it helps prevent subsequent coalescence of drops, thus stabilizing the emulsion. Surfactant-induced coalescence suppression is a means of kinetic trapping, i.e., a metastable emulsion morphology may persist for long periods,

because drops cannot coalesce and allow the emulsion to evolve into a more preferred morphology. Therefore, surfactants offer a powerful method of controlling the morphology and phase continuity in oil/water systems. In particular, by carefully controlling the emulsion-preparation protocol, it is possible to realize kinetically-trapped emulsion morphologies that are different from the preferred morphology.

For over a decade, it has been known that some polymeric surfactants (henceforth, called “compatibilizers”) can suppress coalescence in blends of immiscible homopolymers.<sup>3–8</sup> This raises the intriguing possibility of applying ideas of structure control from oil/water emulsions to immiscible polymer blends. In particular, can we employ a compatibilizer and some specific blending protocol to control the structure and phase continuity in a polymer blend, and realize a morphology different from the preferred one?

That the morphology of polymer blends can be varied via the blending protocol has been shown previously (see, for example, Baker and Scott<sup>9</sup> as well as several more articles cited in the Results section). All of the previous research was

This article contains supplementary material available via the Internet at <http://www.interscience.wiley.com/jpages/0001-1541/suppmat>.

Correspondence concerning this article should be addressed to S. Velankar at [velankar@pitt.edu](mailto:velankar@pitt.edu).

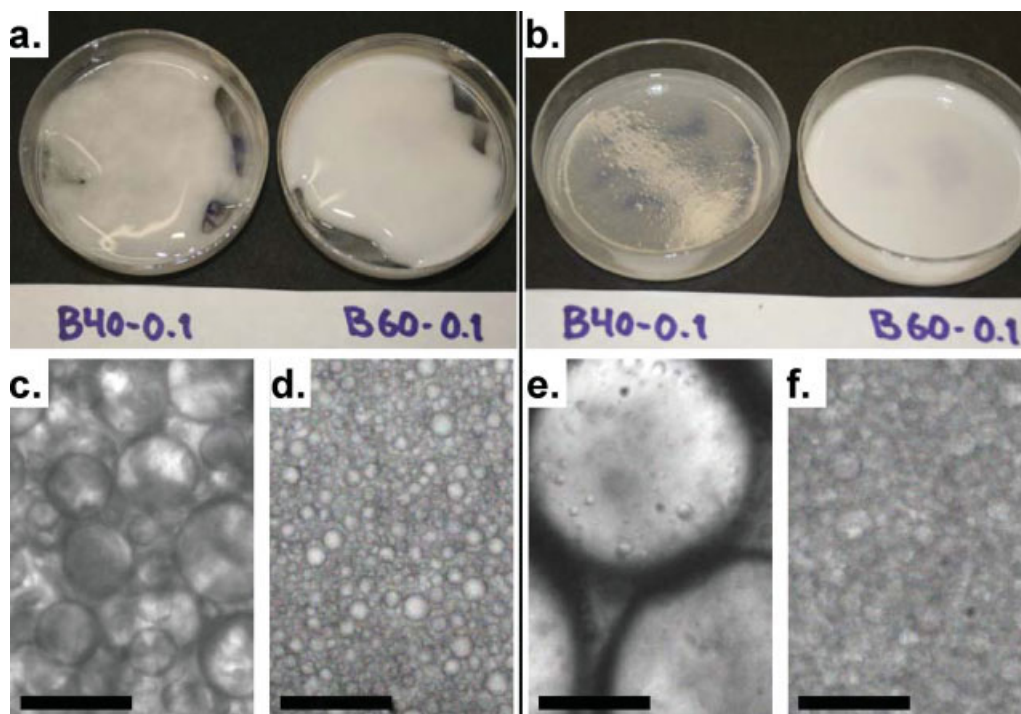


**Figure 1.** Petridishes containing B40-0.1 and B60-0.1 before (a), and after (b) two weeks under quiescent conditions. c-f.: Corresponding optical microscope images. Scale bars represent 20 microns.

[Color figure can be viewed in the online issue, which is available at [www.interscience.wiley.com](http://www.interscience.wiley.com).]

conducted in relatively complex systems: commercial polymers were used, the compatibilizer was generated by an interfacial chemical reaction, and there was a complex interplay between blending kinetics and interfacial reaction kinetics. In this article, we examine morphology control in a much simpler “model” experimental system.

The blends are composed of polydimethylsiloxane (PDMS) and polyisobutylene (PIB), with a diblock copolymer of PIB and PDMS added as compatibilizer; we recently showed that this diblock copolymer can suppress the coalescence of PDMS drops in PIB.<sup>10</sup> This experimental system is simpler than the previous research in many ways: all components are liquid at room-temperature (allowing hand-blending), are optically transparent, and allow long-term morphological stability tests without thermal degradation. The compatibilizer has a simple structure (diblock), and its concentration can be controlled precisely since it is added and not reactively-generated. Finally, only a small amount (0.1 wt%) of compatibilizer is added, which ensures that all the effects of compatibilizer are interfacial, and bulk effects are negligible. We explore possibilities of applying preparation protocols devised for oil/water emulsions to control the morphology and phase continuity in this “model” immiscible polymer blend system.

## Materials and Methods

The blends under investigation consisted of polydimethylsiloxane (PDMS, Rhodorsil 47V60000 from Rhodia Chemicals, MW roughly 150,000 g/mol) and polyisobutylene (PIB 32, Soltex Chemicals, MW roughly 1300 g/mol). Both components are liquid at 25°C and nearly Newtonian ( $\eta_{\text{PDMS}} = 56.2$  Pa.s and  $\eta_{\text{PIB}} = 57.3$  Pa.s at 25°C), with PDMS having

a relaxation time on the order of 0.01 s and PIB even smaller. The well-matched viscosity of PIB and PDMS implies a drop viscosity ratio of almost exactly 1. All rheological experiments were conducted at 25°C, whereas all blending and microscopy were conducted at room temperature without any temperature control.

A diblock copolymer of PIB and PDMS ( $M_{w,\text{PIB}} = 6,150$  g/mol and  $M_{w,\text{PDMS}} = 8,000$  g/mol,) was used as a compatibilizer. This same diblock has been used in previous studies.<sup>10–13</sup>

As previously,<sup>10</sup> since we are interested in questions of phase continuity, we control the volume fractions (rather than weight fractions) of the PIB and PDMS. However, since the density of the compatibilizer is not known exactly, it is still convenient to control the compatibilizer on a weight basis. Accordingly, samples will be designated by  $B\phi_{\text{PIB}}-w_{\text{comp}}$ , where  $\phi_{\text{PIB}}$  is the volume fraction of PIB on a compatibilizer-free basis, and  $w_{\text{comp}}$  is the overall weight % of compatibilizer. Samples have up to 0.5 wt. % compatibilizer, and previously we had verified that such small levels of compatibilizer do not affect the bulk rheology of the two phases.<sup>11</sup> For consistency, mixtures of PDMS and compatibilizer (without any PIB) will be designated  $B0-w_{\text{comp}}$ , and mixtures of PIB and compatibilizer (without any PDMS) will be designated  $B100-w_{\text{comp}}$ .

All blends were prepared by hand-mixing the appropriate amounts of compatibilizer and bulk materials with a spatula in a petridish, followed by degassing in vacuum. Unlike our previous articles, the exact sequence in which the two homopolymers and the compatibilizer are blended is crucial here, and will be described in detail in the Results section.

Phase continuity was tested as described previously:<sup>10</sup> briefly, a small amount of blend placed on the tip of a bent wire was immersed in low molecular weight silicone oil,

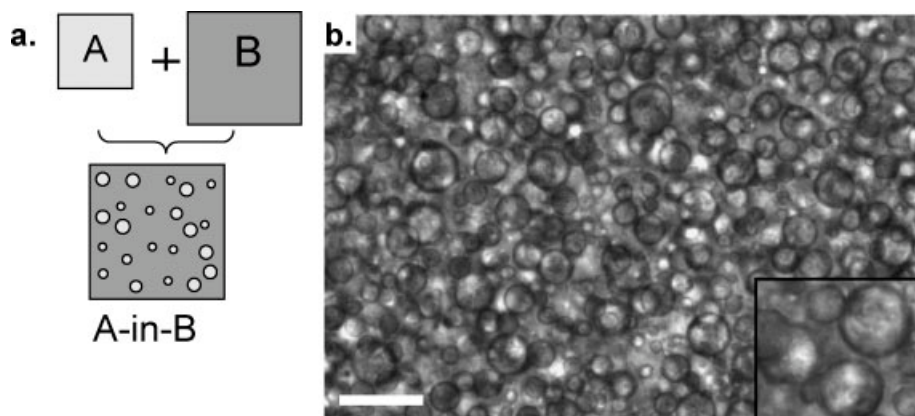


**Figure 2. (a) Standard single-blending procedure, and (b) A B20-0.1 blend with a simple PIB-in-PDMS morphology realized by single-blending.**

Scale bar represents 20  $\mu\text{m}$  for the main image and 10  $\mu\text{m}$  for the inset.

which is miscible with PDMS. If the droplets started dispersing gradually and the sample rose off the wire as a “plume”, it was regarded as PDMS-continuous. In contrast, if the sample stayed intact on the wire, the PIB was taken to be the continuous phase.

Samples were examined with an Olympus CKX-41 inverted microscope in brightfield transmission mode without temperature control and images were recorded with a Basler A302 area scan camera.

Rheological experiments were performed in a TA Instruments AR2000 stress-controlled rheometer using a 40 mm dia/1° cone and plate geometry and a Peltier cell to maintain the sample temperature at 25°C.

## Results

### *Coalescence suppression and phase continuity*

Before evaluating the effect of blending protocol on blend morphology, we will first review two observations from previous research<sup>10</sup> relevant here. The first concerns phase continuity: we found that regardless of the presence or absence of compatibilizer, the minority species would always become the dispersed phase. This observation is in accordance with past research that shows that for blends of equiviscous homopolymers, the phase inversion composition corresponds to a 50/50 blend.<sup>14</sup>

The second observation concerns coalescence suppression. Figure 1 shows photographs of petridishes containing B40-0.1 and a B60-0.1 blends before and after quiescent annealing for two weeks. Immediately after blending (Figure 1a), both blends appeared opaque white due to scattering of light from the drops. After two weeks of quiescent annealing, the B60-0.1 retained its uniformly opaque white appearance. In contrast, after two weeks, the B40-0.1 appeared much less white, with areas of the petridish appearing translucent (less light scattering, indicating larger drops), and “lenses” of the lower density PIB were evident floating on the surface (Figure 1b). Optical microscopy confirmed that the drops of the B40-0.1 blend grew significantly (compare Figure 1c vs. Figure 1e), whereas those of the B60-0.1 grew only slightly (compare Figure 1d vs. Figure 1f). These qualitative observations are the clearest indication that the compatibilizer suppresses quiescent coalescence when PIB is the continuous

phase, but not when PDMS is the continuous phase. The same is true of flow-induced coalescence.<sup>10</sup>

The reasons for the asymmetric effect of the compatibilizer on coalescence are not entirely clear, but a much more detailed discussion was presented previously.<sup>10</sup> In this article, we are only concerned with the experimentally-observed fact of coalescence suppression, and not the underlying causes.

### *Double emulsion morphologies*

Figure 2a shows the standard “single-blending” procedure for blending together two immiscible fluids A and B, along with a small amount of any surface-active species. This same procedure was used in all of our previous research. We applied this procedure to the B20-0.1 blend: the two homopolymers and the compatibilizer were weighed into a petridish and blended with a spatula. As mentioned previously, the minority phase always becomes the dispersed phase in this blend system; indeed optical microscopy revealed the PIB-in-PDMS droplet-matrix morphology of Figure 2b. (Note that Figure 2b by itself does not indicate whether the drops are PIB or PDMS, however, the continuous phase has been verified to be PDMS using the procedure described previously.<sup>10</sup>)

Figure 3a illustrates an alternate “double-blending” protocol for blending together the same components. In the first step, the phase A is blended with only a small portion of phase B. Since B is a minority, a B-in-A morphology is expected. This blend is then itself blended with the remaining B to realize a B-in-A-in-B “double emulsion” morphology. We applied this double-blending procedure to the PIB/PDMS system. In the first step, a B60-0.1 blend with a PDMS-in-PIB morphology (Figure 3b) was prepared by single-step blending. It was then blended in a 1:2 ratio with B0-0.1 (i.e., PDMS with 0.1% compatibilizer) so as to realize a blend whose overall composition was identical to the B20-0.1 of Figure 2b. The resulting morphology (Figure 3c) was, however, dramatically different from Figure 2b: the PIB drops had a significant number of PDMS subdrops. Realizing such a PDMS-in-PIB-in-PDMS double emulsion morphology requires that the inner PDMS drops do not “leak” out during blending, and hence the second blending step involved only gentle blending.

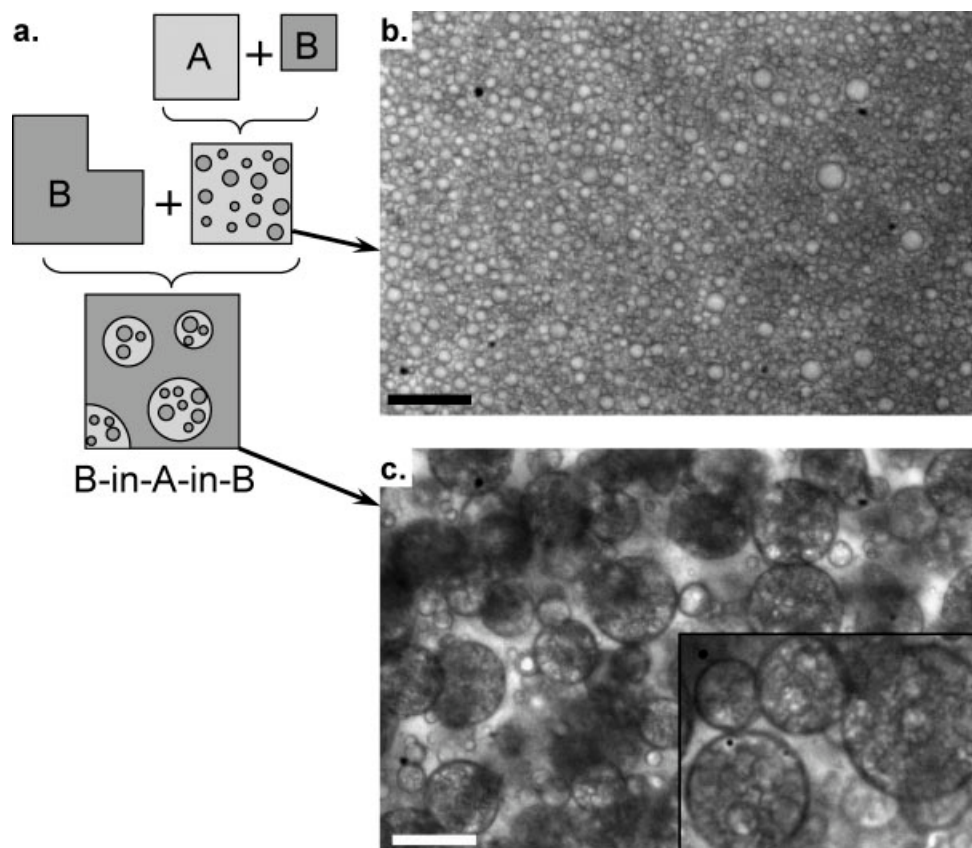


**Figure 3. (a) Double-blending procedure; (b) A B60-0.1 blend with a PDMS-in-PIB morphology, and (c) A B20-0.1 blend prepared by gently blending b. with B0-0.1 (i.e., PDMS with 0.1% compatibilizer).**

Scale bars represent 20  $\mu\text{m}$  for the main images, and 10  $\mu\text{m}$  in the inset to c.

The double blending procedure to realize double emulsion morphologies is well-known in the literature on oil/water emulsions, and such double emulsions have been considered for controlled release of pharmaceuticals or food compounds.<sup>15–17</sup> The double blending procedure has also been used in the polymer melt-blending literature. To our knowledge, all such cases employed reactive compatibilization, and the relatively large amount of graft copolymer compatibilizer formed may have had significant bulk effects.<sup>18–20</sup> In contrast, here we have shown that a simple diblock copolymer, even added in a sufficiently small quantity to be an interfacial modifier but cause no bulk effects (akin to a surfactant in an oil/water system), can achieve a stable double emulsion morphology.

There are also some other methods of realizing a double emulsion morphology. Subdrops can sometimes occur spontaneously when melt-blending immiscible polymers.<sup>21–25</sup> This is believed to occur when the majority component has a higher melting temperature, causing a phase inversion during the blending process,<sup>26</sup> or due to rapid coalescence of the dispersed phase which engulfs some of the matrix phase as subdrops.<sup>19,25</sup> Apart from melt blending, the double-emulsion morphology is also very common in impact-modified polystyrene, or other rubber-toughened glassy plastics. In those cases, it is often called a “salami” morphology.<sup>27–29</sup> Such a PS-in-rubber-in-PS morphology is achieved not by a melt blending procedure, but by phase

inversion occurring during polymerization. In such cases, a large fraction of graft copolymer is essential to observe a salami structure. A double emulsion morphology was also obtained due to thermodynamic interactions between the block copolymer and the homopolymers.<sup>30</sup> In this case samples were solvent-cast, and contained a far larger quantity (15%) of block copolymer.

Coalescence suppression is crucial to realizing a double emulsion morphology. We applied the double blending procedure to two systems in which coalescence of the subdrops is not suppressed. The first is a compatibilizer-free version of Figure 3, i.e., a B60-0 sample was prepared and then blended with additional PDMS, so as to realize a final composition of B20-0 (Figure 4a). The second is an inverted version of Figure 3: A B40-0.1 blend with a PIB-in-PDMS morphology was first prepared and was then blended with a B100-0.1 (i.e., PIB with 0.1% compatibilizer) to prepare a B80-0.1 sample (Figure 4b). In both cases, the subdrops readily coalesced with each other. Many of these large subdrops also coalesced with the external matrix, but some survived the blending process. Therefore, some of the external drops in Figure 4a and b, especially in Figure 4b, show a single large subdrop. In summary, subdrop coalescence must be suppressed to realize a stable double emulsion morphology.

However, coalescence suppression by itself is not sufficient to realize a double emulsion morphology. It is also essential that the second blending step be done gently. If the

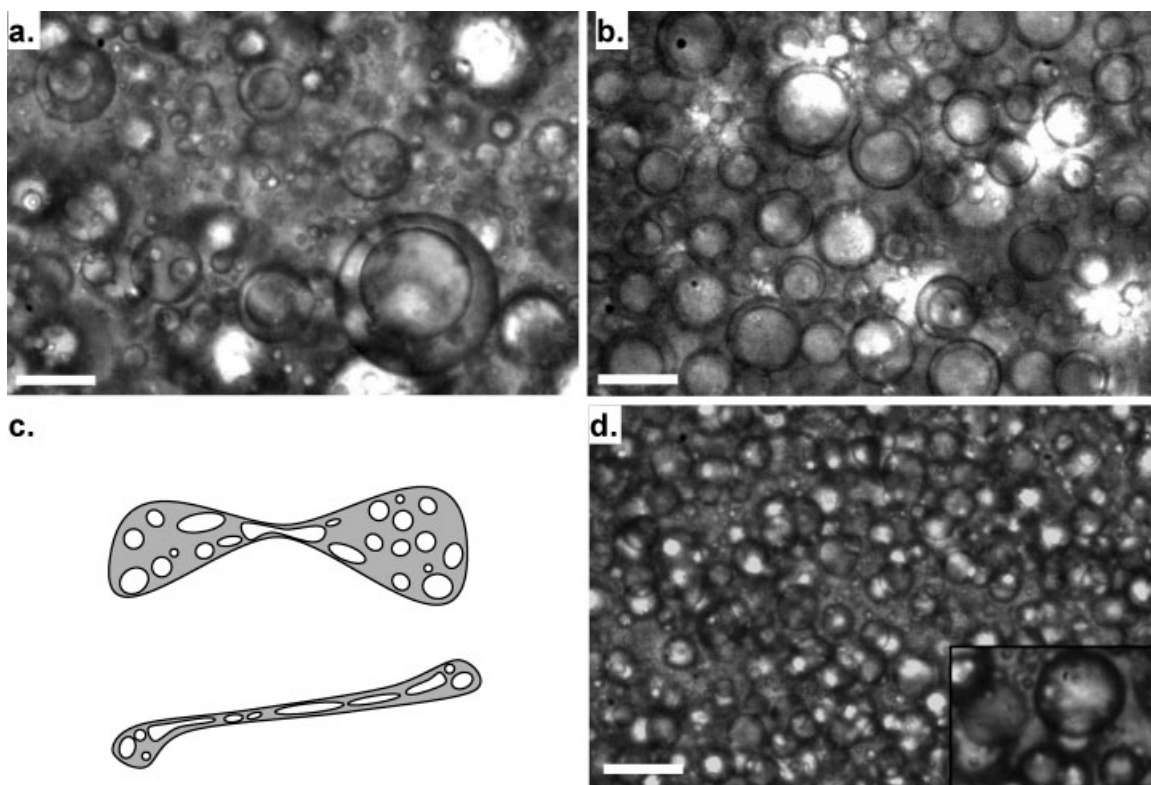


**Figure 4. Double emulsion morphologies are unstable if compatibilizer is absent, compatibilizer does not suppress coalescence, or if the double emulsion is blended vigorously: (a) B20-0 prepared by gently blending B60-0 with PDMS, (b) B80-0.1 prepared by gently blending B40-0.1 and B100-0.1, (c) Double emulsion drops deforming when subjected to vigorous blending; some subdrops are likely to leak out during deformation and breakup, and (d) The blend of Figure 3c, subjected to vigorous blending.**

Scale bars represent 20 microns for the main images, and 10 microns for the inset to d.

second blending is vigorous, the large stresses induce breakup of double emulsion drops (shown in Figure 4c), and can lead to substantial leakage of subdrops. This can be illustrated by subjecting the B20-0.1 double emulsion of Figure 3c to vigorous blending; in this case, virtually all drops leaked out into the continuous phase during blending, and a simple droplet/matrix morphology resulted (Figure 4d). There is also a significant decrease in drop-size upon vigorous blending (Figure 3c vs. Figure 4d), which is attributable to two causes: (1) the near-complete leakage of subdrops, which can explain at most 16% decrease in diameter (corresponding to 40% decrease in volume), and (2) breakup induced by the vigorous blending. The fact that vigorous blending induces substantial leakage is also well-known in the oil/water emulsion literature; indeed, standard procedures call for using a high-shear homogenizer when preparing the first emulsion, but only gentle stirring when dispersing this emulsion into additional drop-phase fluid.<sup>17</sup> In the polymer literature as well, it has been recognized that extended blending, especially at the high stresses typical of polymer extrusion, can destroy a double emulsion morphology.<sup>20</sup> Therefore, it is important to limit the blending time to preserve the double emulsion morphology. An alternate approach is to simultaneously crosslink either the drops or the subdrops so that leakage is not strongly suppressed.<sup>23</sup> Finally, we note that it is difficult to quantitatively judge the extent of leakage from

optical microscopy. Images such as Figure 4a, b and d show hardly any subdrops, and hence massive amounts of leakage can be readily inferred. However, images, such as Figure 3c are more difficult to evaluate: it is not clear whether the drops of blend of Figure 3c have an internal subdrop volume fraction of 0.4 (same as Figure 3b), or whether some leakage occurred, and the internal subdrop volume fraction is less than 0.4. One of the goals of the following section is to investigate whether rheology can be used more quantitatively to estimate the leakage.

#### *Rheological properties of double emulsions*

The rheological properties of B20-0.1 samples prepared by the double-blending procedure depend on the intensity of blending; the more gentle the blending, the larger is the fraction of subdrops that survive the blending process. Therefore, we will illustrate the range of rheological behavior possible by showing results for two specific B20-0.1 samples, one blended gently (same sample as Figure 3c, henceforth, denoted B20-0.1g), and the other blended extremely vigorously (same sample as Figure 4d, henceforth, denoted B20-0.1v). These two samples will be compared against the reference case of the single-blended B20-0.1 sample.

Figure 5 compares the storage modulus  $G'$  and the magnitude of the complex viscosity  $|\eta^*|$  of these three samples; we

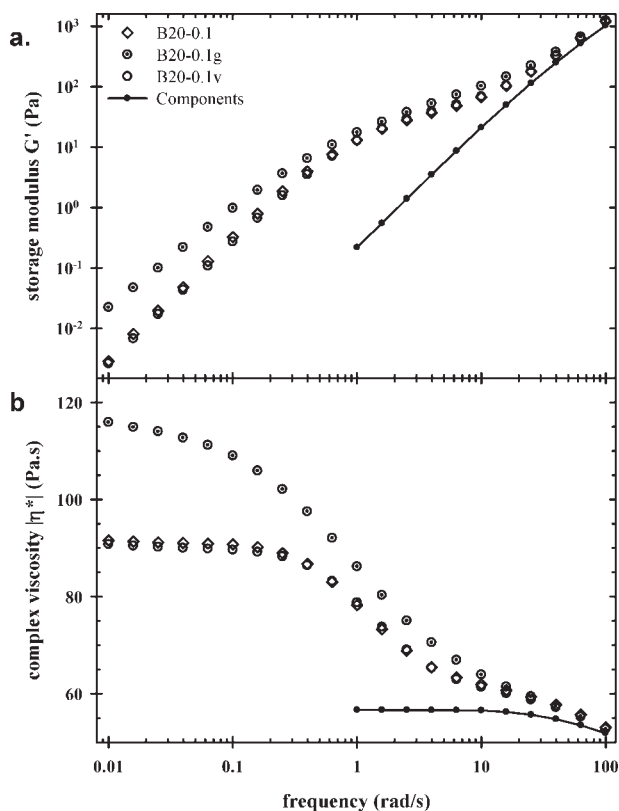


**Figure 5. Dynamic oscillatory properties of various blends ‘as-loaded’ in the rheometer. The ‘components’ curve is a volume-weighted average of the PIB and PDMS homopolymers.**

emphasize that all three have the *same overall composition*, but only differ in their preparation method. These measurements were conducted on “as-loaded” samples with no additional shearing. All blends show qualitatively similar behavior: at high-frequencies, the properties approach the volume-weighted average of the components, whereas at low-frequencies, the blends show an additional relaxation process which is manifested as a pronounced shoulder in  $G'$ , and an increase in the terminal complex viscosity. In the case of uncompatibilized blends, this “interfacial relaxation process” is attributable to the deformation and relaxation of drop shapes due to the applied oscillatory flow.<sup>31–33</sup> In compatibilized blends, the interfacial relaxation is attributable to both drop shape relaxation, as well as relaxation of gradients in interfacial tension on the drop interfaces.<sup>6,10,34</sup>

Figure 5 makes two noteworthy observations. First, the terminal complex viscosity of the double-blended B20-0.1g is substantially larger than that of the single-blended B20-0.1. Second, the rheological properties of the B20-0.1v blend are comparable to the single-mixed B20-0.1, as is indeed expected from the almost complete leakage of the subdrops noted by microscopy (Figure 4d). We also note that the  $G'$  of the B20-0.1g blend is substantially higher than of the other two blends, especially at low frequencies. This is likely attributable to the very large drop size caused by gentle blending, rather than to the double emulsion morphology *per se*.

In Martin and Velankar,<sup>10</sup> we used the shear protocol of Figure 6a to examine the effect of stress on various rheologi-

cal properties. Here, we will apply the same shear protocol to the three B20-0.1 samples prepared by various methods, and compare their rheological properties. The shear protocol consists of steady shearing at a specific stress for 2,000 strain units, followed by strain recovery after cessation of shear, followed by an oscillatory frequency sweep at 25% strain under quiescent conditions. These three steps are repeated at successively lower stresses. Optical microscopy of blends recovered from the rheometer at the end of this test sequence shows that the double emulsion morphology persists under shear, i.e., subdrop leakage is not obviously evident. A further comment on this will be made when discussing Figure 7a.

The steady shear viscosities of the blends,  $\eta$ , obtained at each stress are shown in Figure 6b (read off the right axis). The relative viscosity,  $\eta_r$ , is obtained by normalizing the viscosity with the volume-weighted average of the components<sup>10</sup>

$$\eta_r = \frac{\eta}{\phi_{\text{PIB}}\eta_{\text{PIB}} + \phi_{\text{PDMS}}\eta_{\text{PDMS}}} \quad (1)$$

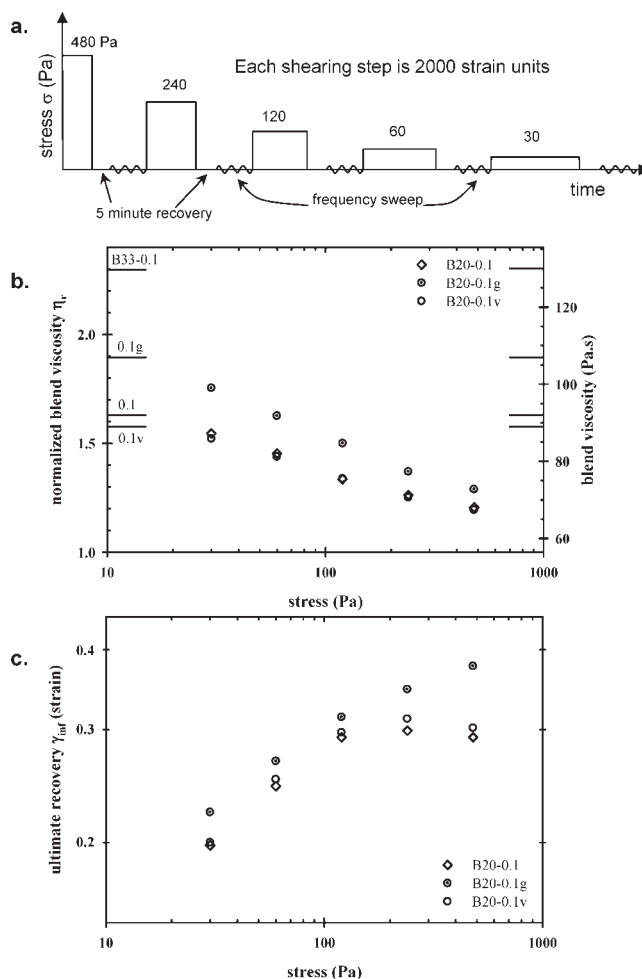


**Figure 6. (a) Shear history used in rheological experiments, (b) Viscosity (symbols) and terminal complex viscosity (horizontal lines), and (c) Ultimate recovery. Note that the y-axis in c. is logarithmic.**

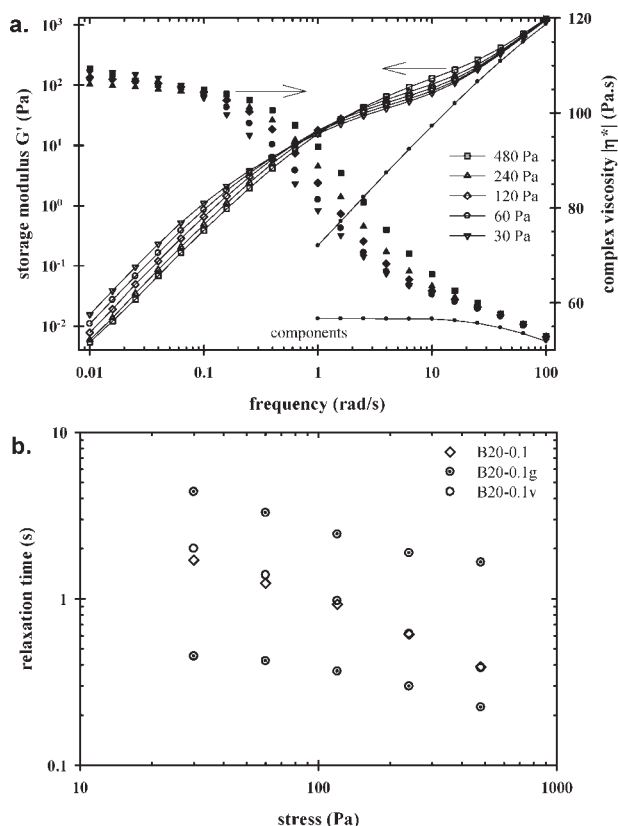


**Figure 7. (a) Storage modulus and magnitude of the complex viscosity for B20-0.1g after shearing at each stress, and (b) Relaxation times obtained from the oscillatory data.**

Note that the PIB and PDMS have nearly equal viscosities, and hence in the above equation, the denominator  $\approx \eta_{\text{PIB}} \approx \eta_{\text{PDMS}}$ . The values of the relative viscosity are shown in Figure 6b on the left axis. All three blends are seen to be shear-thinning. The reasons for the shear-thinning have been discussed previously: with increasing stress, the drops deform and orient along the flow direction, and the contribution of interfacial tension gradients to the shear stress also decreases.<sup>11</sup> The chief observation of Figure 6b is that the viscosity of B20-0.1g double emulsion morphology is significantly higher than of the other two blends at all stresses.

Upon cessation of steady shear, blends show strain recovery. Recovery is attributable to the shape-recovery of initially-deformed drops,<sup>35,36</sup> as well as to the relaxation of interfacial tension gradients along the drop surfaces.<sup>13,37</sup> The strain vs. time curves during recovery for the present blends resembled those shown previously.<sup>13</sup> As previously, the kinetics of recovery cannot be captured by a single time constant,<sup>36,38</sup> and therefore it is convenient to characterize the recovery in terms of only one quantity, the ultimate recovery  $\gamma_{\infty}$ . The ultimate recovery for the three blends is shown in Figure 6c. The ultimate recovery decreases with decreasing stress as noted previously for blends with a higher volume fraction of drops.<sup>10</sup> The chief observation is that the B20-0.1g blend has slightly higher recovery than the other two blends.

The dynamic oscillatory data for the double-blended B20-0.1g taken after shearing at each stress are shown in Figure

7a. The data for the other two blends are not shown but resemble the data of Figure 7a. The chief effect of shearing is an increase in the time scale (decrease in the characteristic frequency) of the interfacial relaxation process. The time scale of the interfacial relaxation scales with the drop-size, and hence Figure 7a indicates an increase in the size of the external PIB drops due to coalescence. (The PDMS subdrops are not expected to coalesce as mentioned at the beginning of the Results section, and indeed, optical microscopy of samples withdrawn from the rheometer at the end of the test sequence shows no obvious change in subdrop size). As previously<sup>10</sup> we will extract two quantities from the oscillatory data: the terminal complex viscosity  $|\eta_0^*|$ , and the terminal relaxation time.

The terminal complex viscosity can be obtained directly from the low-frequency data. Figure 7a shows that the terminal complex viscosity did not change significantly with shearing, and in particular, it did not decrease systematically. As discussed later in this article, the terminal complex viscosity is the best indicator of whether or not the subdrops leak out. Thus, the fact that  $|\eta_0^*|$  does not reduce with extended shearing ( $10^4$  strain units in the shear protocol of Figure 6a) is a strong indication that subdrops are stable against leakage under shear flow, at least up to 200 Pa stress. The average value of  $|\eta_0^*|$  at all five stress levels is plotted as horizontal lines in Figure 6b (read off the right axis).  $|\eta_0^*|$  can also be normalized in the same fashion as Eq. 1, and the corresponding value of the relative terminal complex viscosity, denoted  $|\eta_{0r}^*|$ , can be read off the left axis in Figure 6b. The chief observation is that the B20-0.1g has a significantly higher terminal complex viscosity than the other two blends.

The detailed procedure for extracting the terminal relaxation time has been described previously; briefly, the viscoelastic contribution of the bulk is subtracted from the measured  $G'$  data, and the results are fitted to a sum of a small number of Maxwell modes. For the single-blended B20-0.1 blend and the B20-0.1v blend, only a single Maxwell mode was adequate to capture the interfacial relaxation process accurately. For the B20-0.1g sample, two modes were necessary, presumably due to the broad (nearly bimodal) drop-size distribution inherent in double emulsion morphologies. Sample fits to the oscillatory data are shown in the Supplementary Material (Figure 9). The terminal relaxation times thus obtained are plotted in Figure 7b. The chief observation is that the double emulsion blend B20-0.1g has a much higher terminal relaxation time than the other two blends.

From an examination of Figures 6 and 7, the following comments can be made. First, all the rheological properties of the double-blended B20-0.1v blend are close to those of the single-blended sample, thus quantitatively proving the nearly complete absence of subdrops in the vigorously-blended sample. Thus, in the limit of vigorous blending, the rheological properties of the double-blended samples are identical to those of the single-blended sample.

The gently-blended B20-0.1g sample may be regarded as the other limit. The rheological properties of B20-0.1g are qualitatively similar to the simple droplet-matrix blends, however, quantitatively, B20-0.1g has a higher terminal complex viscosity, higher steady shear viscosity, higher relaxation time, and slightly higher ultimate recovery. These quantitative differences may, at the simplest, be interpreted by

regarding the B20-0.1g double emulsion morphology as a simple droplet-matrix morphology, but with an effective drop volume fraction  $\varphi_{\text{eff}} > \varphi_{\text{PIB}} = 0.2$ , and an effective drop viscosity ratio exceeding 1. This immediately suggests using the rheology to estimate the effective volume fraction, and therefore, the extent of leakage. Of the properties displayed in Figures 6 and 7, the steady shear viscosity, strain recovery, and relaxation time all depend on the applied stress and on the drop size. In contrast, since the terminal complex viscosity is expected to be independent of drop size and stress, it may be best-suited for estimating the  $\varphi_{\text{eff}}$ , and hence the extent of leakage. Unfortunately, leakage of subdrops affects the terminal complex viscosity of the blend in several different ways: (1) most directly, leakage decreases the volume fraction of the drops, thus, reducing the blend viscosity; (2) leakage also reduces the effective drop viscosity ratio of the drops (as the subdrop volume fraction decreases). This also indirectly reduces the viscosity of the double emulsion,<sup>39</sup> and (3) Leakage may also redistribute the compatibilizer, raising the amount of compatibilizer adsorbed on the interface of the outer drops. This may raise the terminal complex viscosity. For all these reasons, it is not possible to use the magnitude of the terminal complex viscosity to quantitatively estimate extent of leakage. Qualitatively, however,  $|\eta_0^*|$  is still an excellent indicator of the stability of the double emulsion morphology against leakage of subdrops. For example, comparing B20-0.1g from Figure 5b (as-loaded sample) vs. Figure 7a (sheared sample),  $|\eta_0^*|$  is seen to reduce after the first shearing step of 480 Pa, but then remain nearly constant. This is indicative of some leakage in the very first shearing step (perhaps as the initially-large drops breakup when sheared for the first time), but no further leakage on extended shearing at lower stresses.

Finally, it is interesting to compare the measured  $|\eta_0^*|$  against that expected in the limiting case in which none of the subdrops leak out. The B20-0.1g blend was prepared by blending B60-0.1 and B0-0.1 in a 1:2 ratio. In the absence of any subdrop leakage, the volume fraction of the PDMS subdrops is  $0.4 \times 0.333 = 0.133$ . Accordingly, the effective volume fraction of the drops  $\varphi_{\text{eff}} = 0.2 + 0.133 = 0.333$ , i.e., the viscosity of such a zero-leakage double emulsion should be comparable to that of a B33-0.1 blend. (In fact, the viscosity may be even higher since the double-emulsion drops, which are comprised of the B60-0.1 blend, now have an effective drop viscosity ratio of about 4).<sup>10</sup> Figure 6b, however, shows that the zero-shear viscosity of the B20-0.1g double emulsion is substantially lower than of a B33-0.1 blend, indicating that even the gently-mixed B20-0.1g blend had significant leakage. Thus, although the optical image of Figure 3c shows the presence of numerous subdrops, the rheological results suggest that gentle blending did not completely prevent leakage.

### High-dispersed phase blends

The previous sections have shown that one specific emulsion preparation protocol, viz. double blending, can be applied successfully to polymer blends. It is then natural to consider other preparation protocols known from oil/water systems which may realize different morphologies. One well-known example from oil/water systems involves adding the

dispersed phase in a *gradual* fashion into the continuous phase in the presence of an emulsifier. This procedure, which we call “multistep concentration” (Figure 8a), can yield a high-dispersed phase morphology i.e., one in which the drop-volume fraction significantly exceeds 0.5. Multistep concentration is the basis of recipes<sup>40</sup> for home-made mayonnaise that require that oil be added drop-wise into an aqueous phase containing egg yolk, so as to result in an oil-in-water emulsion of high-oil fraction (typically over 65%), and hence a “creamy” consistency. If oil is not added drop-wise but all at once, a water-in-oil emulsion results. Also similar to the previous double-blending case, it is crucial that the emulsifier prevent coalescence of oil drops, a role played by an egg yolk protein, lecithin.<sup>41</sup> If coalescence occurs, the emulsion will phase-invert into a water-in-oil mayonnaise with a “runny” consistency.

We implemented the multistep concentration procedure in PIB/PDMS blends to examine whether a high-dispersed phase morphology could be realized. The experimental protocol was chosen such that a B20-0.1 sample would be prepared by gradual addition of pure PDMS to a compatibilizer/PIB mixture. Accordingly, the starting point was a B100-0.5 blend, i.e., 0.5wt% mixture of the compatibilizer in the PIB. In the first blending step, 0.228 g of PDMS was blended vigorously with 0.779 g of B100-0.5, resulting in 1.01 g of a PDMS-in-PIB blend with  $\varphi_{\text{PIB}} = 0.78$ . As per the notation of this article, this sample is designated B78-0.41. In the second step, an additional 0.16 g of PDMS was added and blended vigorously. This process was continued with roughly 0.2  $\pm$  0.04 g of PDMS being added in each step. An accurate determination of phase continuity is critical in this experiment, and hence the following protocol was devised for testing the phase continuity after each blending step: a small drop of the blend was placed on a glass slide and a drop of pure PIB was placed adjacent to it. As the two drops spread on the slide, they contacted each other. Phase continuity could be unambiguously determined from this experiment: with a PDMS-in-PIB morphology, no interface was evident once the two drops contacted each other. The sequence of images collected after each blending step is shown in Figure 8b–g. It is clear that a high-dispersed phase morphology was not realized at all; after the fifth blending step (i.e., transition from Figure 8e to 8f), when  $\varphi_{\text{PDMS}}$  increased to 0.56, the blend phase-inverted into a PDMS-in-PIB-in-PDMS double emulsion morphology. This phase inversion was confirmed contacting the blend with a PIB drop as described previously; a sharp interface between the blend, and the PIB confirms that the blend has PDMS as its continuous phase. Upon further addition of PDMS, when  $\varphi_{\text{PIB}} = 0.4$ , virtually all subdrops leaked out due to the vigorous blending, and the rheological properties of this sample (not shown) were virtually identical to those of the corresponding single-mixed PIB-in-PDMS B40 blend.<sup>10</sup>

We have conducted the aforementioned experiment with some variations: placing the compatibilizer in the PDMS phase being added gradually (rather than in the phase PIB present at the beginning), and adding the drop phase in finer increments in each blending steps. The results were identical: (1) when the PIB volume fraction decreased below 50%, the PDMS-in-PIB morphology was lost, and (2) full phase inversion with negligible subdrops was evident at  $\varphi_{\text{PIB}} = 0.4$ .



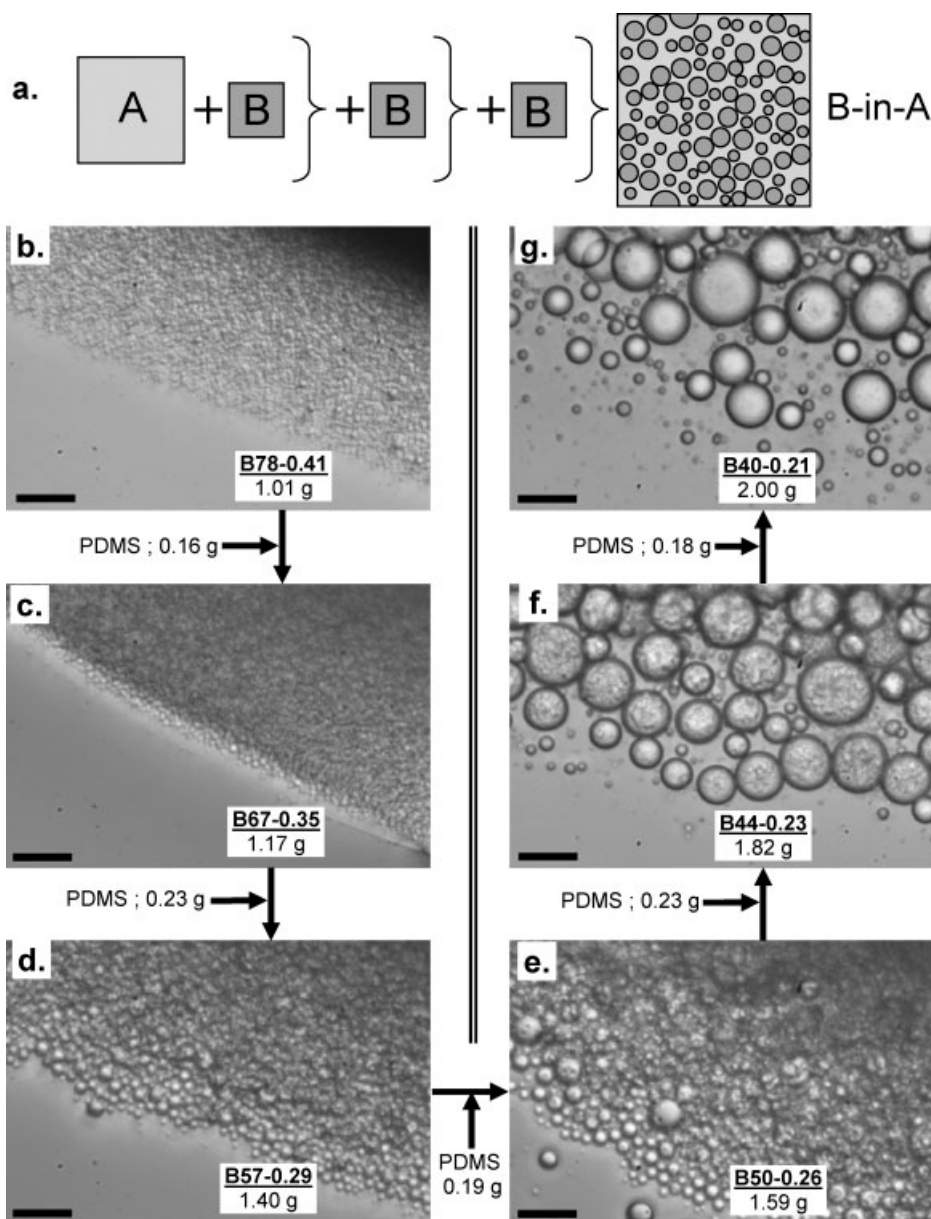


**Figure 8. (a) ‘Multistep concentration’ protocol, and (b–g) Sequence of samples realized during multistep concentration.** Each blend results from blending pure PDMS with the previous blend. Scale bars represent 20  $\mu\text{m}$ .

Bouchama et al.<sup>42</sup> have noted that in oil/water systems, exceedingly small changes in the overall composition—drop volume fraction changing by  $O(10^{-3})$  in each blending step—may be necessary to extend the phase inversion to higher drop volume fractions. In our case, that would correspond to additions of mg-quantities of PDMS in each blending step, not possible experimentally.

The type of phase inversion relevant here—viz. that induced by changing the relative volume fraction of the two phases—is generally called a “catastrophic” phase inversion in the oil/water emulsion literature. Ostwald’s theory is generally recognized as the earliest model of phase inversion.<sup>43,44</sup> Ostwald suggested that phase inversion occurs when the volume fraction of the dispersed phase approaches close packing (0.74 for monodisperse drops; higher for poly-

disperse drops). Certainly, the volume fraction at phase inversion of 0.5 observed in Figure 8 is far from close packing. More sophisticated theories of phase inversion account for the thermodynamics of the emulsion using catastrophe theory,<sup>45</sup> or the competitive kinetics of drop breakup and coalescence.<sup>46,47</sup> Yet, these explanations are phenomenological and do not address the mechanism whereby inversion occurs. Specifically, if the coalescence of PDMS drops in PIB is suppressed, why did the additional PDMS added in step 5 not get dispersed as drops, but instead become the continuous phase?

While we are unable to answer this question in detail, it is important to note one general aspect of the multistep concentration procedure, viz. with every successive step, the fresh PDMS being added must be blended with a blend of an increasing (and, therefore more mismatched) viscosity. For

example, in step 5, the PDMS was blended with B50-0.26 whose zero-shear viscosity was at least four-fold larger.<sup>10</sup> It is well-known that in two-phase systems with a large viscosity difference, the phase inversion composition is shifted toward the low-viscosity component, i.e., the low-viscosity component becomes the continuous phase when it is still in a minority.<sup>14</sup> Accordingly, the additional PDMS added in step 5 has a tendency to encapsulate the higher-viscosity blend, thus forming a double emulsion. Upon continued blending, the double emulsion subdrops can leak out as illustrated in Figure 4c. Such leakage is then responsible for the complete phase inversion into a simple PIB-in-PDMS morphology. Indeed, in the oil/water emulsion literature, phase inversion is sometimes accompanied by an intermediate double emulsion structure.<sup>42,46,48,49</sup>

## Summary and Closing Comments

A compatibilizer can sometimes suppress coalescence of drops in a polymer blend. In such cases, it is possible to exploit coalescence suppression to control the blend morphology. In this article, we have compared three blending procedures: one simple procedure used in all of our previous research, and two more complex procedures drawn from the literature on oil/water emulsions.

The simple procedure, dubbed single-step blending, requires that all components be added together and blended at once. This procedure always yields a simple droplet-matrix morphology with the minority phase being the dispersed phase.

In the double blending procedure, a droplet/matrix blend is first prepared and then dispersed into additional drop phase fluid. In oil/water emulsions, this can give rise to a drop-within-drop morphology, called a double emulsion. We show that a double emulsion morphology can be realized in polymer blends as well, provided the second blending step is conducted gently. Rheological properties of the double emulsion morphology qualitatively resemble those of a simple droplet-matrix morphology, but with a higher effective drop volume fraction, and a higher effective drop viscosity ratio.

Finally, the multistep concentration procedure consists of adding the drop phase in a gradual fashion, rather than all at once, into the dispersed phase. In oil/water systems, such a procedure can yield a high-dispersed phase emulsion. In the polymer blend case, we were unsuccessful in realizing a high-dispersed phase morphology; phase inversion occurred when the drop-volume fraction exceeded 0.5. The multistep concentration procedure inevitably involves blending two fluids with highly mismatched effective viscosities and we speculate that this viscosity mismatch is responsible for the phase inversion.

The central hypothesis of this research was that the precise sequence in which various components are blended affects the two-phase morphology. This is well-established in the oil/water emulsion literature, and has also been demonstrated in a few limited cases in blends of commercial polymers using reactive compatibilization. Here we have shown that the same ideas can be applied in much simpler model polymer systems: it appears that even a simple diblock copolymer compatibilizer, added at only 0.1wt% loading can achieve the same effects provided it can stop coalescence. We have

tested only two blending protocols here, but many others may be devised to modify the morphology. Even variations of the two protocols considered here can significantly modify the morphology. For example, a simple variation of the double-blending protocol is to add all the compatibilizer in the first step and none in the second step (instead of distributing the compatibilizer in both blending steps as done in Figure 3). We implemented this variation i.e. blended B60-0.3 with pure PDMS to realize a B20-0.1 blend. We found that the initial B60-0.3 blend was composed of much finer PDMS drops, thus, the final double emulsion morphology had subdrops that were much smaller than in Figure 3c. It is easy to conceive of other variations that would also affect the morphology, e.g., blend the initial A-in-B emulsion into additional A in a gradual fashion (instead of all-at-once as done here), blend the initial A-in-B emulsion itself in a gradual fashion. Changing the overall concentration of compatibilizer would offer even more possibilities for morphology control.

## Acknowledgments

We are grateful to the Laboratory of Applied Rheology at the Katholieke Universiteit Leuven for making the PIB-PMDS diblock copolymer available for this research, and Rhodia Silicones and Soltex Chemicals for providing the PDMS and PIB homopolymers respectively. We thank Dr. Alejandro Peña and an anonymous reviewer for directing us to some of the literature on double emulsions in oil/water and polymer/polymer systems. This research was supported by a NSF-CAREER grant CBET0448845, and an NSF-IREE grant CBET-0637019 from the National Science Foundation, USA.

## Literature Cited

1. Sjöblom J, ed. *Encyclopedic handbook of emulsion technology*. New York: Marcel Dekker; 2001.
2. Binks BP, ed. *Modern Aspects of Emulsion Science*. Cambridge: Royal Society of Chemistry; 1998.
3. Sundararaj U, Macosko CW. Drop breakup and coalescence in polymer blends: The effects of concentration and compatibilization. *Macromolecules*. 1995;28:2647–2657.
4. Milner ST, Xi H. How copolymers promote mixing of immiscible homopolymers. *J Rheol*. 1996;40:663–687.
5. Van Puyvelde P, Velankar S, Moldenaers P. Rheology and morphology of compatibilized polymer blends. *Curr Opin Coll Int Sci*. 2001;6:457–463.
6. Van Hemelrijck E, Van Puyvelde P, Velankar S, Macosko CW, Moldenaers P. Interfacial elasticity and coalescence suppression in compatibilized polymer blends. *J Rheol* 2004;48:143–158.
7. Hudson SD, Jamieson AM, Burkhardt BE. The effect of surfactant on the efficiency of shear-induced drop coalescence. *J Coll Int Sci*. 2003;265:409–421.
8. Lyu S, Jones TD, Bates FS, Macosko CW. Role of block copolymers on suppression of droplet coalescence. *Macromolecules*. 2002; 35:7845–7855.
9. Baker W, Scott C, Hu GH, eds. *Reactive polymer blending*. Chapters 4 and 5. Cincinnati: Hanser Gardner; 2001.
10. Martin J, Velankar S. Effects of compatibilizer on immiscible polymer blends near phase inversion. *J Rheol*. 2007;51:669–692.
11. Velankar S, Van Puyvelde P, Mewis J, Moldenaers P. Steady-shear rheological properties of model compatibilized blends. *J Rheol*. 2004;48:725–744.
12. Velankar S, Van Puyvelde P, Mewis J, Moldenaers P. Effect of compatibilization on the breakup of polymeric drops in shear flow. *J Rheol*. 2001;45:1007–1019.
13. Wang J, Velankar S. Strain recovery of model immiscible blends: Effects of added compatibilizer. *Rheol Acta*. 2006;45:741–753.
14. Paul DR, Barlow JW. Polymer blends (or alloys). *J of Macromolecular Sci, Reviews in Macromolecular Chemistry*. 1980; C18:109–168.

15. Buezzello K, Muller BW. Emulsions as drug delivery systems. In: F. Nielloud and G. Marti-Mestres. *Pharmaceutical Emulsions and Suspensions*. New York: Marcel Dekker; 2000.
16. Salager JL. Formulation concepts for the emulsion maker. In: F. Nielloud and G. Marti-Mestres. *Pharmaceutical Emulsions and Suspensions*. New York: Marcel Dekker; 2000.
17. Garti N, Benichou A. Double emulsions for controlled release applications - Progress and Trends. In: J. Sjoblom. *Encyclopedic Handbook of Emulsion Technology*. New York: Marcel Dekker; 2001.
18. Pagnouille C, Jerome R. Particle-in-particle morphology for the dispersed phase formed in reactive compatibilization of SAN/EPDM blends. *Polymer*. 2001;42:1893–1906.
19. Martin P, Maquet C, Legras R, Bailly C, Leemans L, van Gurp M, van Duin M. Particle-in-particle morphology in reactively compatibilized poly(butylene terephthalate)/epoxide-containing rubber blends. *Polymer*. 2004;45:3277–3284.
20. Favis BD, Lavallee C, Derdouri A. Preparation of composite dispersed phase morphologies in incompatible and compatible blends during melt processing. *J of Mat Sci*. 1992;27:4211–4218.
21. Ban LL, Doyle MJ, Disko MM, Smith GR. Morphology of ethylene-co-propylene rubber-modified nylon 66 blends. *Polym Communications*. 1988;29:163–166.
22. Favis BD, Chalifoux JP. The effect of viscosity ratio on the morphology of polypropylene/polycarbonate blends during processing. *Polym Eng Sci*. 1987;27:1591–1600.
23. Martin P, Maquet C, Legras R, Bailly C, Leemans L, van Gurp M, van Duin M. Conjugated effects of the compatibilization and the dynamic vulcanization on the phase inversion behavior in poly(butylene terephthalate)/epoxide-containing rubber reactive polymer blends. *Polymer*. 2004;45:5111–5125.
24. Sundararaj U. Morphology development during polymer blending. University of Minnesota; 1994. Ph.D. Thesis.
25. Pagnouille C, Koning C, Leemans L, Jerome R. Reactive compatibilization of SAN/EPR blends. 1. Dependence of the phase morphology development on the reaction kinetics. *Macromolecules*. 2000;33:6275–6283.
26. Sundararaj U, Macosko CW, Shih CK. Evidence for inversion of phase continuity during morphology development in polymer blending. *Polym Eng Sci*. 1996;36:1769–1781.
27. Wagner ER, Robeson LM. Impact polystyrene: factors controlling the rubber efficiency. *Rubber Chem Tech*. 1970;43:1129–1137.
28. Sperling LH. In: L. H. Sperling. *Recent advances in polymer blends, grafts, and blocks*. New York: Plenum press; 1974.
29. Schierholz JU, Hellmann GP. In situ graft copolymerisation: salami morphologies in PMMA/EP blends: part I. *Polymer*. 2003;44:2005–2013.
30. Adedeji A, Jamieson AM, Hudson SD. Phase inversion in compatibilized immiscible polymer blends with exothermic interfacial mixing. *Macromolecules*. 1995;28:5255–5261.
31. Graebing D, Muller R, Palierne JF. Linear viscoelasticity of incompatible polymer blends in the melt in relation with interfacial properties. *J De Physique Iv*. 1993;3:1525–1534.
32. Oldroyd JG. On the formulation of rheological equations of state. *Proc Roy Soc Lon A*. 1950;200:523–541.
33. Palierne JF. Linear rheology of viscoelastic emulsions with interfacial tension. *Rheol Acta*. 1990;29:204–214.
34. Oldroyd JG. The effect of interfacial stabilizing films on the elastic and viscous properties of emulsions. *Proc Roy Soc Lon*. 1955; A232:567–577.
35. Gramespacher H, Meissner J. Melt elongation and recovery of polymer blends, morphology, and influence of interfacial tension. *J Rheol*. 1992;41:27–44.
36. Vinckier I, Moldenaers P, Mewis J. Elastic Recovery of immiscible blends 1. Analysis after steady state shear flow. *Rheol Acta*. 1999;38:65–72.
37. Velankar S, Zhou H, Jeon HK, Macosko CW. CFD evaluation of drop retraction methods for the measurement of interfacial tension of surfactant-laden drops. *J Coll Int Sci*. 2004;272:172–185.
38. Wang J, Velankar S. Strain recovery of model immiscible blends without compatibilizer. *Rheol Acta*. 2006;45:297–304.
39. Choi SJ, Schowalter WR. Rheological properties of non-dilute suspensions of deformable particles. *Phys Fluids*. 1975;18:420–427.
40. Rombauer Becker M, Becker E, Rombauer IS. *Joy of Cooking*. New York: Scribner; 1997.
41. McGee H. *On food and cooking : the science and lore of the kitchen*. New York: Scribner; 2004.
42. Bouchama F, van Aken GA, Autin AJE, Koper G. On the mechanism of catastrophic phase inversion in emulsions. *Coll Surf A*. 2003;231:11–17.
43. Ostwald W. Beitrage zur Kenntnis der Emulsionen. *Kolloid Zeitschrift*. 1910;6:103.
44. Salager JL, Marquez L, Pena AA, Rondon M, Silva F, Tyrode E. Current phenomenological know-how and modeling of emulsion inversion. *Ind Eng Chem Res*. 2000;39:2665–2676.
45. Salager JL. Phase transformation and emulsion inversion on the basis of Catastrophe theory. In: P. Becher. *Encyclopedia of Emulsion Technology*. New York: Marcel Dekker; 1983.
46. Nienow AW. Break-up, coalescence and catastrophic phase inversion in turbulent contactors. *Adv in Colloid and Interface Sci*. 2004;108-09:95–103.
47. Davies JT. A quantitative kinetic theory of emulsion type. I. Physical chemistry of the emulsifying agent. *Proc. Intern. Congr. Surface Activity, 2nd, London, 1957*. 1957;1:426–438.
48. Pacek AW, Nienow AW, Moore IPT. On the structure of turbulent liquid-liquid dispersed flows in an agitated vessel. *Chem Eng Sci*. 1994;49:3485–3498.
49. Brooks BW, Richmond HN. Phase inversion in nonionic surfactant oil-water systems. 2. Drop size studies in catastrophic inversion with turbulent mixing. *Chem Eng Sci*. 1994;49:1065–1075.

Manuscript received July 11, 2007, and revision received Nov. 13, 2007.